Conductive atomic force microscopy study of single molecule electron transport through the Azurin-gold nanoparticle system

Samuele Raccosta, Chiara Baldacchini, Anna Rita Bizzarri, and Salvatore Cannistraro

Citation: Appl. Phys. Lett. **102**, 203704 (2013); doi: 10.1063/1.4807504
View online: http://dx.doi.org/10.1063/1.4807504
View Table of Contents: http://apl.aip.org/resource/1/APPLAB/v102/i20
Published by the American Institute of Physics.

Conductive atomic force microscopy study of single molecule electron transport through the Azurin-gold nanoparticle system

Samuele Raccosta,[1] Chiara Baldacchini,[1,2] Anna Rita Bizzarri,[1] and Salvatore Cannistraro[1,a)]
[1]*Biophysics & Nanoscience Centre, DEB-CNISM, Università della Tuscia, I-01100 Viterbo, Italy*
[2]*Institute of Agro-environmental and Forest Biology, National Research Council, I-05010 Porano (TR), Italy*

(Received 13 February 2013; accepted 6 May 2013; published online 21 May 2013)

Transduction of biorecognition events into electrical signals through integration of single redox metalloproteins in bioelectronic nanodevices requires both a reliable electrical contact between the biomolecule and the metallic electrode and an efficient overall conduction mechanism. These conditions have been met in the hybrid system obtained by linking gold nanoparticles on top of Azurin proteins, in turn assembled on gold surfaces. Such an assembling strategy, combined with a conductive atomic force microscopy investigation, has allowed us to put into evidence an unprecedented matching between current and topography features and to attribute the intramolecular charge transport to a non-resonant tunnelling mechanism. © *2013 AIP Publishing LLC*.
[http://dx.doi.org/10.1063/1.4807504]

Redox metalloproteins have emerged as promising candidates for the development of bioelectronic devices, owing to their electron transfer, catalytic and recognition properties.[1] Their nanoscale dimension, along with the very fast and efficient electron transport capability, opens the possibility of using these proteins as sensitive elements for biosensors. These hybrid systems, being able to transduce a biological event into an electrical signal, could find application in ultra-high sensitive detection of chemical and biological markers in environmental and clinical diagnostics.[2] In this respect, it is crucial to achieve both an efficient electrical contact among the biomolecules and the electrodes[3] and an adequate control of the electron transport properties of the hybrid system,[4] even at single biomolecule level.

An efficient coupling entails a minimization of the contact resistance between the biomolecules and the electrodes. Covalent bonds may provide suitable contacts because are highly reproducible, quite stable, and facilitate an efficient electron transport.[5] Indeed, coupling with flat gold electrodes have been achieved through chemical bonds between gold atoms and metalloprotein groups (thiols, disulfides, and amines).[6–12]

Concerning the electron transport through the protein milieu, several mechanisms can be invoked such as hopping, through-space, and through-bond tunnelling,[4,13,14] according to distances and pathways travelled by charge carriers; this aspect being crucial to exercise a precise control of the electron conduction through the overall system.

Recently, use of gold nanoparticles (GNPs) conjugated with biomolecules resulted extremely beneficial, both to improve the electrical contact with the electrodes[15,16] and to modulate the conduction, also via an enhancement of the local electromagnetic field.[17] In particular, this has been observed by scanning tunnelling microscopy (STM) and cyclic voltammetry on hybrid systems involving redox metalloproteins.[18–20] However, since the current-voltage (I-V) curves acquired by STM involve a contribution from the air gap between the electrodes and refers to the electronic density of states of both tip and sample, the intramolecular conduction mechanism can be somewhat obscured.

To circumvent such a drawback, conductive atomic force microscopy (C-AFM) can be used. It establishes, through a force feedback control, a tuneable electrical contact between tip and sample, allowing one to simultaneously acquire the surface topography and the corresponding current map.[21] Nevertheless, soft biomolecules generally require strong applied forces to draw a sizable current, with consequent structure deformation and low image resolution.

By using C-AFM, we have revisited the electron transfer properties of the redox metalloprotein Azurin (AZ), previously assembled on Au electrodes, after linking a 5 nm GNP on its top (GNP/AZ/Au), as sketched in Fig. 1. This assembling strategy, if compared with the simple AZ/Au system, achieves more stable and enhanced currents at lower applied forces, resulting in an unprecedented good matching between topography and current maps. Moreover, I-V curves are consistent with both a current transmission coefficient between tip and biomolecule almost equal to unity and a non-resonant tunnelling intramolecular conduction.

AZ from Pseudomonas Aeruginosa (Sigma Chemical Co.) was deposited on freshly annealed gold substrates (Arrandee®) by incubation with a protein solution (10–30 μM in 50 mM ammonium acetate at pH 4.10, for 12 h at 4 °C). Sample quality was checked by means of Contact Mode AFM (CMAFM) in aqueous solution (Nanoscope IIIa/Multimode SPM Digital Instruments, 12 μm scanner, and silicon nitride probes with 10 nm radius of curvature and 0.02 N/m spring constant).

Fig. 2(a) shows a typical CMAFM image of an AZ/Au sample, displaying a dense layer of proteins with a surface roughness of about 0.44 nm, in agreement with previous results.[6] Stable images have been acquired upon consecutive scans, on different areas, demonstrating that biomolecules

a)Author to whom correspondence should be addressed. Electronic mail: cannistr@unitus.it. Tel./Fax: +39 0761 357136.

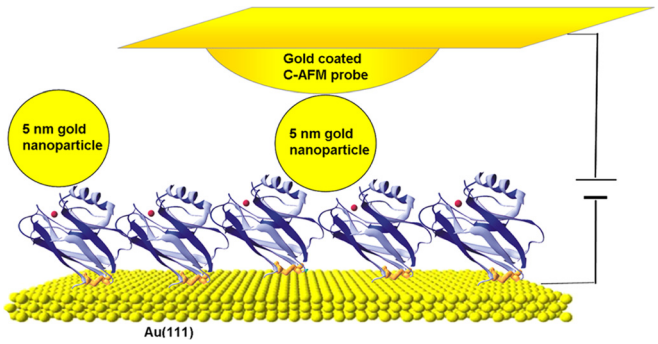

FIG. 1. Schematic illustration (not in scale) of 5 nm GNPs linked to the top of an AZ monolayer self-assembled on an Au substrate and contacted by an Au-coated C-AFM probe.

are uniformly and robustly bound to the surface. The firm linking of AZ molecules occurs presumably via spontaneous breaking of its disulphide bridge in proximity of the gold surface and consequent formation of S-Au chemical bonds,[8,22] with retention of AZ functionality both in fluid[8] and in air[9] environment (hydration water being present in the latter case[23]). A smaller number of molecules might be also immobilised via exposed amine groups.[24]

To verify the presence of single AZ layers on the substrates, 200×200 nm areas have been raster scanned at high force load, carefully controlled in order to remove the softer protein layer without damaging the gold surface (Fig. 2(b)): a mean scratching depth of 2.3 ± 0.3 nm has been obtained (Fig. 2(c)), consistently with AZ height on gold.[6]

Then, a drop of GNPs (Ted Pella, 5.0×10^{13} particles/ml, 5.5 nm nominal diameter, variation coefficient<15%) has been deposited on the AZ/Au samples (for 1 h, at room temperature).

Fig. 2(d) shows a typical CMAFM image of a GNP/AZ/Au sample (as that sketched in Fig. 1). Individual GNPs, homogeneously distributed on the AZ monolayer, are clearly discerned. Topography images are stable and reproducible, with no evidence of GNP mobility on protein surface upon multiple scans, indicating that they are robustly bound. The vertical size of single GNPs (4.9 ± 0.8 nm) well matches with their nominal diameter, while the much larger lateral size (17 ± 2 nm) is due to tip radius convolution. CMAFM scratching procedure has been repeated on these samples (Fig. 2(e)) and a mean hole depth of 6.9 ± 1.2 nm (Fig. 2(f)) has been obtained; this being consistent with the sum of AZ and GNP heights, indicating that GNPs are bound on top of the protein monolayer, presumably through a covalent interaction between AZ exposed amine groups and GNP uncoordinated atoms.[24]

Current and force imaging in air was performed on GNP/AZ/Au samples by a C-AFM equipment (PicoLE Molecular Imaging, Inc., current sensing module of $\sigma = 1$ nA/V, gold coated cantilevers with 50 nm tip radius and 0.05 N/m spring constant). Typical C-AFM topography and current maps are shown in Fig. 3. C-AFM topography (Fig. 3(a)) is much blurred with respect to that shown in Fig. 2(d), likely due to three main factors: (i) adhesion occurrence due to the formation, in air, of a water meniscus between tip and sample destabilizing the force control and enlarging the effective contact area; (ii) larger C-AFM tip with respect to standard AFM tips, due to the metal coating (50 nm vs 10 nm), increasing the effect of tip radius convolution on nanoscale features; (iii) applied bias introducing an electrostatic interaction between probe and substrate, thus causing that effective applied force does not match with force set-point.[15] C-AFM current map (Fig. 3(b)) shows bright spots, stable upon

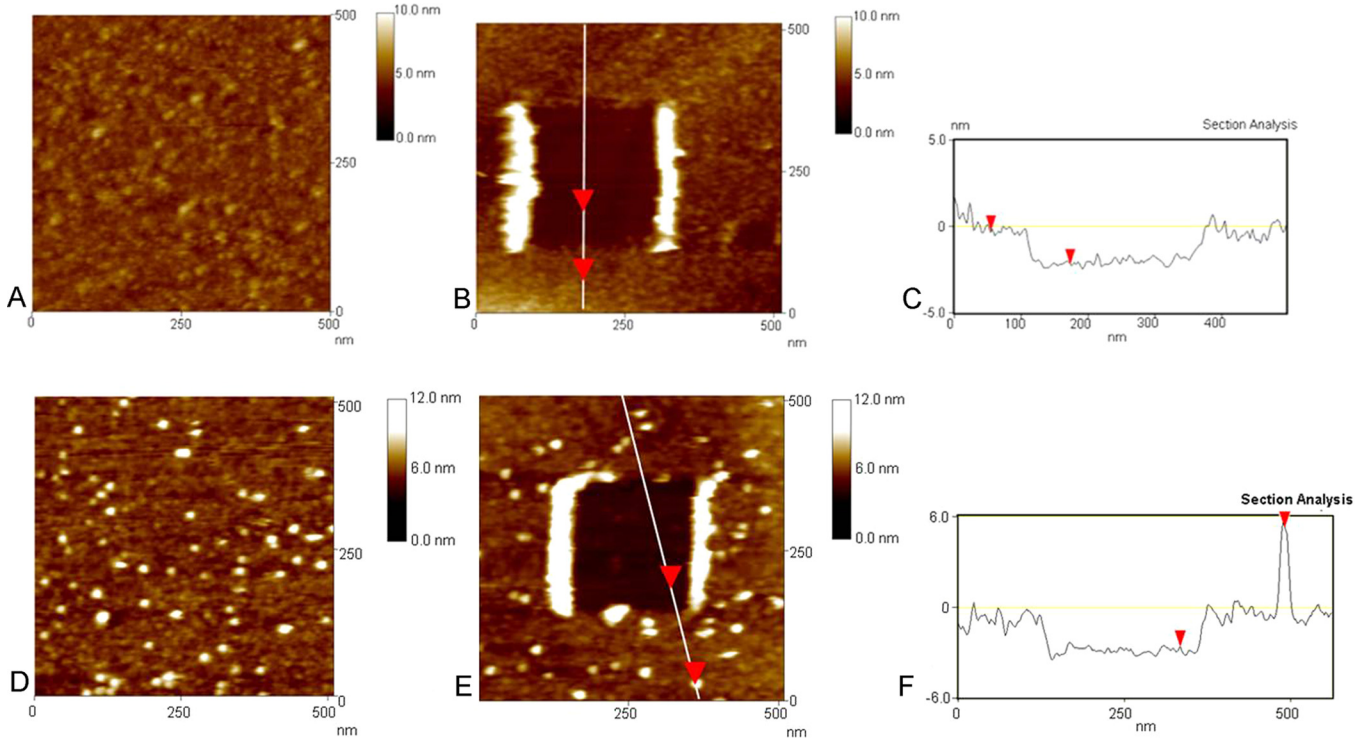

FIG. 2. CMAFM images acquired in aqueous solution: AZ monolayer on the Au substrate before (a) and after (b) the scratching procedure, together with the cross section profile (c) taken along the line through the scratched area; AZ monolayer on Au substrate with GNPs linked on top before (d) and after (e) the scratching procedure and cross section profile (f) taken along the line through the scratched area.

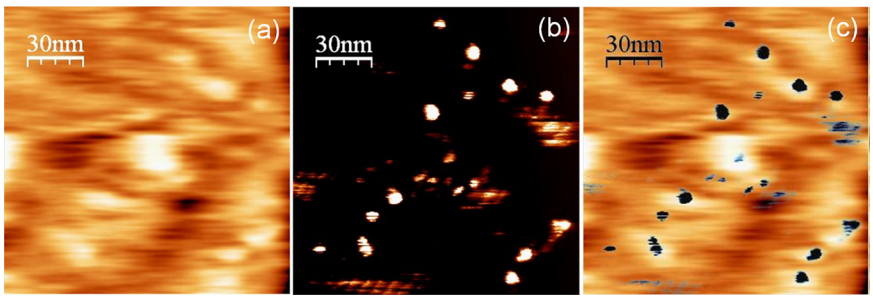

FIG. 3. C-AFM images acquired in air (F = 2.0 nN; V = 1.0 V; tip grounded; Au-coated tip with k = 0.05 N/m) of an AZ monolayer on Au after linking GNPs on its top: (a) CMAFM topography (vertical scale: 15 nm); (b) simultaneous current signal (vertical scale: 1 nA); (c) negative current image superimposed on topography map.

consecutive scans, with 3–6 nA intensity at 1.0 V bias and 2 nN load. Notwithstanding the low quality of topography, the superimposition of topography and current images (Fig. 3(c)) shows a spatial correspondence between the topographic bumps and the current spots.

Because the C-AFM current maps acquired at 1.0 V bias and 2 nN load from AZ/Au samples show only very few, blurred conductive regions with current intensities lower than 100 pA (data not shown), the highly conductive features observed on the GNP/AZ/Au samples, and the related topographic bumps, are very likely ascribable to GNPs on top of the AZ monolayer, that enables sizable current to be measured through the contact with the C-AFM tip.

To further investigate the conduction across the single tip-GNP-AZ-Au nanojunction, I-V spectroscopy experiments have been carried out: I-V curves have been recorded at selected sites of the current images (single I-V sweep between ±2 V in 0.5 s). The overall drift in x-y plane, evaluated to be less than 1 Å/s, did not substantially affect the tip position during measurements. A current fluctuation of about 1 pA/s has been observed by recording the current without any feedback.

Representative I-V curves obtained by positioning the C-AFM tip on the current spots displayed by the highly conductive samples (tip-GNP-AZ-Au) and on the protein monolayer without GNPs (tip-AZ-Au) are shown in Fig. 4 (circles and triangles, respectively). When the tip contacts a GNP at 2 nN load, very reproducible I-V curves are obtained, with a current response of 3–6 nA at +1 V bias. Instead, when the tip is placed on the AZ monolayer, no current response is detected in the ±2 V range unless the applied load is increased up to 14 nN. At such high load, instable I-V curves with current responses in the 0–100 pA range at +1 V bias are obtained. Such behaviour is confirmed by the junction resistance values obtained by linearly fitting the I-V curves around zero applied bias (represented by the inverse of the slope). A resistance $R = 50 \pm 5 \times 10^9\ \Omega$ has been measured for tip-GNP-AZ-Au nanojunctions, while a much higher value is inferred from the tip-AZ-Au I-V curves (almost flat around zero bias). A similar improvement of the electrical coupling in hybrid nanojunctions has been recently observed after conjugating cytochrome c molecules with metallic carbon nanotubes: the current measured by C-AFM across the proteins increases of one order of magnitude,[25,26] while the nanojunction resistance decreases from $10^{12} - 10^{10}$ to $4 \times 10^9\ \Omega$.[26]

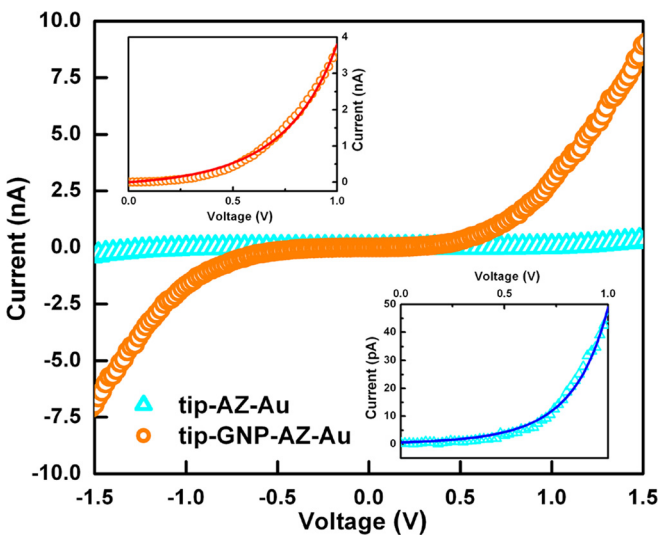

FIG. 4. Representative I-V curves and fitting examples for a tip-GNP-AZ-Au nanojunction at 2 nN applied load (circle marks, top inset) and for a tip-AZ-Au nanojunction at 14 nN applied load (triangle marks, bottom inset).

All these evidences clearly indicate that a good and reliable electron conduction through the AZ monolayer is obtained only when proteins are conjugated with GNPs. Due to the relative ratio of GNP and AZ diameters, every single GNP could contact 1 to 3 AZ molecules, if a full coverage is assumed for the AZ monolayer. However, the I-V curves measured on top of several GNPs are very stable and reproducible, suggesting that charge carriers travel through the protein milieu by choosing the shortest travel path, independently from the number of molecules contacted by the GNP.

Then, to disclose further details on the conduction mechanisms across our AZ-based nanojunctions, the I-V curves have been analyzed within a transport model based on non-resonant tunneling,[27] under the assumption that only one AZ molecule is involved in the transport process and that its redox centre does not mediate the transport through resonant tunneling processes. This latter assumption is suggested by the absence of resonance features in the I-V curves,[28] as expected for AZ molecules at applied bias within the ±2 V range.[29] In this framework, the current has been defined as $I = VG$, where G is the conductance given by the Landauer formula $G = (2e^2/h)T_{tot}$, with e being the electron charge, h the Planck constant and T_{tot} the total electron transmission probability across the nanojunction. T_{tot} is expressed as $T_{tot} = T_{top} \cdot T_{mol} \cdot T_{down}$, to take into account the contributions from charge transmission across the protein (T_{mol}), and across its top (on the tip side, T_{top}) and bottom (on the metal surface side, T_{down}) contacts. T_{mol} is modelled as a coherent non-resonant tunnelling across a rectangular barrier of height Φ and length L: $T_{mol} = \exp[-L(4\pi/h)\ (2\,m^*(\Phi - eV))^{1/2}]$, where V is the applied bias and m^* the effective electron mass (equal to $0.16m$, being m the electron mass). T_{down} have been

assumed equal to unity, as for protein molecules chemisorbed at metal electrodes.[27] T_{top} refers, on one case, to the tip-AZ contact and, on the other, to the tip-GNP contact, and was left as a free fitting parameter. Thus, the I-V curves have been fitted by the final expression $I = V(2e^2/h)\cdot T_{top}\cdot\exp[-L(4\pi/h)(2\,m^*(\Phi - eV))^{1/2}]$, up to +1 V. Two examples of the I-V experimental data fits are shown in the insets of Fig. 4 for both the tip-GNP-AZ-Au (up, left) and tip-AZ-Au (down, right) nanojunctions.

The tunnelling parameters obtained for charge transport through AZ molecules are $\Phi = (0.9 \pm 0.1)$eV and $L = (1.6 \pm 0.2)$nm for tip-GNP-AZ-Au nanojunction (at 2 nN) and $\Phi = (0.8 \pm 0.1)$ eV and $L = (1.8 \pm 0.2)$nm for tip-AZ-Au nanojunction (at 14 nN). These values are comparable, pointing out that the electron transport across AZ is characterized by an identical tunnelling mechanism in both cases, and they are also similar to those previously obtained for metalloproteins on conductive electrodes.[26,28,30]

A significant difference is instead observed in the values of T_{top}: it varies from 10^{-3} to 10^{-1} for tip-AZ-Au nanojunctions, while it is close to unity for tip-GNP-AZ-Au. Low values of T_{top} indicate a weak electrical coupling, that implies a decrement of the overall nanojunction conductance,[27] consistently with the low current signal observed for the AZ/Au system. $T_{top} \approx 1$ indicates that the tip establishes, via the GNP, a very good electrical coupling with the protein, as that occurring between the AZ molecules and the Au substrate. This supports the occurrence of a stable binding between AZ and GNP, as well as the absence of any significant resistance between the tip and the GNP, resulting in a much more efficient electrical conjugation with respect to that achieved by direct tip-AZ contact.

Collectively, these results allow us to conclude that GNPs may provide an efficient top electrical contact to AZ proteins immobilised on a gold substrate, thus enabling to detect a reliable and good electrical current through single molecules and to evidence an unprecedented good matching between C-AFM topography and current maps. Establishing top contact via GNPs represents a suitable strategy to improve the overall conduction mechanism in hybrid nanojunctions, which, on the other hand, can be easily extended to other type of immobilised biomolecules and could help in building up stable GNP/protein/electrode hybrid systems to be exploited in biosensing nanodevices.

This work was partly supported by a grant from the Italian Association for Cancer Research (AIRC, IG 10412) and by a PRIN-MIUR 2009 project (No. 2009WPZM4S). Thanks are due to Dr. Laura Andolfi for her preliminary measurements.

[1]I. Willner and E. Katz, Angew. Chem., Int. Ed. **39**, 1180 (2000).
[2]N. L. Rosi and C. A. Mirkin, Chem. Rev. **105**, 1547 (2005).
[3]H. Haick and D. Cahen, Prog. Surf. Sci. **83**, 217 (2008).
[4]I. Ron, L. Sepunaru, S. Itzhakov, T. Belenkova, N. Friedman, I. Pecht, M. Sheves, and D. Cahen, J. Am. Chem. Soc. **132**, 4131 (2010).
[5]X. D. Cui, A. Primak, X. Zarate, J. Tomfohr, O. F. Sankey, A. L. Moore, T. A. Moore, D. Gust, G. Harris, and S. M. Lindsay, Science **294**, 571 (2001).
[6]L. Andolfi, A. R. Bizzarri, and S. Cannistraro, Thin Solid Films **515**, 212 (2006).
[7]H. A. Heering, F. G. M. Wiertz, C. Dekker, and S. de Vries, J. Am. Chem. Soc. **126**, 11103 (2004).
[8]Q. Chi, J. Zhang, J. U. Nielsen, E. P. Friis, I. Chorkendorff, G. W. Canters, J. E. T. Andersen, and J. Ulstrup, J. Am. Chem. Soc. **122**, 4047 (2000).
[9]W. Li, L. Sepunaru, N. Amdursky, S. R. Cohen, I. Pecht, M. Sheves, and D. Cahen, ACS Nano **6**, 10816 (2012).
[10]L. Andolfi, B. Bonanni, G. W. Canters, M. Ph. Verbeet, and S. Cannistraro, Surf. Sci. **530**, 181 (2003).
[11]L. Andolfi, P. Caroppi, A. R. Bizzarri, M. C. Piro, F. Sinibaldi, T. Ferri, F. Polticelli, S. Cannistraro, and R. Santucci, Protein J. **26**, 271 (2007).
[12]V. E. V. Ferrero, L. Andolfi, G. Di Nardo, S. J. Sadeghi, A. Fantuzzi, S. Cannistraro, and G. Gilardi, Anal. Chem. **80**, 8438 (2008).
[13]H. B. Gray and J. R. Winkler, Biochim. Biophys. Acta **1797**, 1563 (2010).
[14]J. Zhang, A. M. Kuznetsov, I. G. Medvedev, Q. Chi, T. Albrecht, P. S. Jensen, and J. Ulstrup, Chem. Rev. **108**, 2737 (2008).
[15]J. M. Kivioja, K. Kurppa, M. Kainlauri, M. B. Linder, and J. Ahopelto, Appl. Phys. Lett. **94**, 183901 (2009).
[16]I. Ron, N. Friedman, M. Sheves, and D. Cahen, J. Phys. Chem. Lett. **1**, 3072 (2010).
[17]J.-W. Choi, B.-K. Oh, Y.-H. Jang, and D.-Y. Kang, Appl. Phys. Lett. **93**, 033110 (2008).
[18]P. S. Jensen, Q. Chi, F. B. Grumsen, J. M. Abad, A. Horsewell, D. J. Schiffrin, and J. Ulstrup, J. Phys. Chem. C **111**, 6124 (2007).
[19]P. S. Jensen, Q. Chi, J. Zhang, and J. Ulstrup, J. Phys. Chem. C **113**, 13993 (2009).
[20]A. K. Yagati, T. Lee, J. Min, and J.-W. Choi, Bioelectrochemistry **83**, 8 (2012).
[21]Y. Liu, J. He, O. Kwon, and D. M. Zhu, Rev. Sci. Instrum. **83**, 013701 (2012).
[22]A. R. Bizzarri, Biophys. Chem. **122**, 206 (2006).
[23]J. A. Rupley and G. Careri, Adv. Protein Chem. **41**, 37 (1991).
[24]S. Y. Quek, L. Venkataraman, H. J. Choi, S. G. Louie, M. S. Hybertsen, and J. B. Neaton, Nano Lett. **7**, 3477 (2007).
[25]C. Baldacchini, M. A. H. Chamorro, M. Prato, and S. Cannistraro, Adv. Funct. Mater. **21**, 153 (2011).
[26]C. Baldacchini and S. Cannistraro, J. Nanosci. Nanotechnol. **10**, 2753 (2010).
[27]S. M. Lindsay, J. Chem. Educ. **82**, 727 (2005).
[28]J. Zhao, J. J. Davis, M. S. P. Sansom, and A. Hung, J. Am. Chem. Soc. **126**, 5601 (2004).
[29]G. Marruccio, P. Marzo, R. Krahne, A. Passaseo, R. Cingolani, and R. Rinaldi, Small **3**, 1184 (2007).
[30]L. Andolfi, A. R. Bizzarri, and S. Cannistraro, Appl. Phys. Lett. **89**, 183125 (2006).